

Localized Semi-LASER Dynamic ^{31}P Magnetic Resonance Spectroscopy of the Soleus During and Following Exercise at 7 T

Georg B. Fiedler^{† 1,2}, Martin Meyerspeer^{†* 1,2}, Albrecht I. Schmid^{1,2}, Sigrun Goluch^{1,2}, Kiril Schewzow^{1,2}, Elmar Laistler^{1,2}, Arash Mirzahosseini^{3,4}, Fabian Niess^{1,2,5}, Ewald Unger¹, Michael Wolzt⁶, Ewald Moser^{1,2}

[†]equal contribution

¹Center for Medical Physics and Biomedical Engineering,
Medical University of Vienna, Austria

²MR Centre of Excellence, Medical University of Vienna, Austria

³Department of Pharmaceutical Chemistry, Semmelweis University, Budapest, Hungary

⁴Research Group of Drugs of Abuse and Doping Agents, Hungarian Academy of Sciences,
Budapest, Hungary

⁵Graz University of Technology, Institute of Medical Engineering, Austria

⁶Department of Clinical Pharmacology, Medical University of Vienna, Austria

DOI: [10.1007/s10334-015-0484-5](https://doi.org/10.1007/s10334-015-0484-5)

Original version on publisher's website:

<http://link.springer.com/article/10.1007/s10334-015-0484-5>

*Correspondence to:

Martin Meyerspeer, PhD

martin.meyerspeer@meduniwien.ac.at

Center for Medical Physics and Biomedical Engineering

Medical University of Vienna

Lazarettgasse 14

1090 Wien, Austria

+43 (0)1 / 40400 - 64610

Abstract

Object

This study demonstrates the applicability of semi-LASER localized dynamic ^{31}P MRS to deeper lying areas of the exercising human soleus muscle (SOL). The effect of accurate localization and high temporal resolution on data specificity is investigated.

Materials and Methods

To achieve high signal-to-noise ratio (SNR) at a temporal resolution of 6 s, a custom-built calf coil array was used at 7T. The kinetics of phosphocreatine (PCr) and intracellular pH were quantified separately in SOL and gastrocnemius medialis (GM) muscle of 9 volunteers, during rest, plantar flexion exercise and recovery.

Results

The average SNR of PCr at rest was 64 ± 15 in SOL (83 ± 12 in GM). End exercise PCr depletion in SOL ($19 \pm 9\%$) was far lower than in GM ($74 \pm 14\%$). pH in SOL increased rapidly and, in contrast to GM, remained elevated until the end of exercise.

Conclusion

^{31}P MRS in single-shots every 6 s localized in the deeper lying SOL enabled quantification of PCr recovery times at low depletions and of fast pH changes, like the initial rise. Both high temporal resolution and accurate spatial localization improve specificity of Pi and thus pH quantification by avoiding multiple, and potentially indistinguishable sources for changing Pi peak shape.

Keywords: Skeletal Muscle, Phosphocreatine, In Vivo NMR Spectroscopy, Soleus Muscle, Physical Exertion

Introduction

Phosphorus-31 nuclear magnetic resonance spectroscopy (^{31}P MRS) is a well-established, powerful tool for noninvasive measurements of energy metabolism in exercising muscle [1–5]. Particularly, the concentrations and kinetics of phosphorylated creatine (PCr), inorganic phosphate (Pi) and the intracellular pH [6], are accessible, which are directly connected to ATP turnover via the creatine kinase reactions. Numerous dynamic studies have been conducted in the human calf muscle using plantar flexion exercise [2,4], where the main contributing muscles are gastrocnemius medialis (GM), gastrocnemius lateralis (GL) and soleus (SOL), all of which act on the Achilles tendon. GM and GL are located superficially and originate from the lower end of the femur [7]. The deeper lying SOL is connected to tibia and fibula [7], and slightly differs in function. Hence its activation during plantar flexion is also different from the gastrocnemius muscles, the proportion of recruitment depending, amongst others, on the angle of the knee [8]. Based on the differences of these muscles regarding function and anatomy, PCr and Pi kinetics are also expected to differ [9–14]. Acquiring nonlocalized data from a mixture of muscle tissues implies averaging across their respective metabolite concentrations, exchange rates and pH. This degrades sensitivity to small metabolic changes, especially when averaging across muscles with different levels of activation, and does not allow assessing specific metabolic properties from muscles with heterogeneous phenotype (e.g. plantar flexor muscles). This has been confirmed recently, comparing standard nonlocalized MRS of the calf with a volume of interest localized in GM, yielding different results [15]. Within each muscle, on the other hand, activation is relatively homogeneous [16], allowing single-voxel spectroscopy to be applied using a large, anatomy-matched volume.

Several localization schemes for ^{31}P MRS have been used in muscle metabolism studies, the simplest using the limited sensitive volume of a small coil, further methods include ISIS [9,17] DRESS [18], and STEAM [19]. Small coil localization and DRESS cannot monitor deeper lying muscles by virtue, and STEAM inherently loses half the signal [20]. ISIS needs at least eight scans for 3D localization, and with a T_1 of PCr of approximately 4 s at 7 T [21], this results in low temporal resolution. Methods like spectrally selective ^{31}P MRI or chemical shift imaging (CSI) are rapidly advancing. With these methods, several muscles can be measured simultaneously and potential metabolic heterogeneities within a muscle can be detected, however, within their limits of point-spread function, spatial resolution, SNR and temporal resolution. Parasoglou et al. [22] showed the feasibility of 3D ^{31}P MRI to quantify PCr dynamics in the human calf. One serious drawback of this method is that localized pH is not accessible by PCr imaging, which is an important parameter for characterization of aerobic and glycolytic muscle metabolism. CSI, on the other hand, suffers from poor voxel definition and requires far longer acquisition times. While metabolic processes on the order of 20 – 30 seconds have been observed using a gated CSI protocol [14], this approach depends on reproducibly reaching a steady-state (via a known dependence on time, e.g., mono-exponential) and imposes restrictions, e.g., acidosis should not be induced. The semi-LASER single-voxel MRS acquisition scheme is applicable to any exercise intensity and metabolic state, also

any orientation and size of an individual muscle can be covered by the free positioning of the double oblique voxel in three dimensions, provided sufficient B_1 . Further, the contamination by signal from outside of the VOI with the semi-LASER sequence is very low at ca. 1% [20].

The location of SOL, which is covered by the neighboring gastrocnemius muscles, renders data acquisition more challenging. The aim of this study was to acquire accurately localized ^{31}P MR spectra from exercising soleus and to show that it is possible to follow Pi and thus intracellular pH throughout rest, exercise and recovery with a temporal resolution of 6 s, as well as to quantify the PCr recovery time in this muscle via a monoexponential fit.

To our knowledge, this has so far not been demonstrated for ^{31}P MRS localized to a deeper muscle area. To achieve this goal, the combined SNR advances from an ultra-high field scanner, a dedicated, multi-channel calf-coil and an adapted semi-LASER localization scheme were exploited. This extends previous studies (e.g. [15]) by demonstrating that soleus muscle can be monitored under exercise with adequate data quality, comparable to previous results from gastrocnemius.

Materials and Methods

Eleven young healthy subjects (age: 26 ± 5 years, body mass index: $22 \pm 1 \text{ kg/m}^2$, 4 females) were scanned after written informed consent, according to the guidelines of the local ethics committee and the declaration of Helsinki. Nine subjects completed the full protocol with data acquisition in SOL and GM, two subjects were measured for assessment of reproducibility at low PCr depletions in SOL only. An in-house built $^1\text{H}/^{31}\text{P}$ transceive coil array was used in a 7 T whole body MR scanner (Siemens Medical, Erlangen, Germany). The coil consisted of two channels for ^1H and three channels for ^{31}P and was shaped to a half cylinder ($d = 14 \text{ cm}$, $l = 10 \text{ cm}$) to accommodate a human calf [23]. The semi-LASER sequence [20, 24] was applied with a repetition time (T_R) of 6 s. As semi-LASER is a single-shot sequence, this was also the true temporal resolution of the experiment. The shim and the transmit voltage of the RF pulses were adjusted individually for each subject and voxel position, as described previously [20]. The acquisition of spectra from the deeper-lying SOL requires more transmit power (at a given pulse duration) to achieve full adiabatic inversion of the spins, compared to the better studied superficial GM. Limited by the available RF transmit power, the inversion pulse duration was typically $4600 \mu\text{s}$ in SOL ($3400 \mu\text{s}$ for voxels located in GM). The shortest possible echo time (T_E) was selected, which was typically 29 ms for SOL (24 ms for GM). To optimize SNR while ensuring specificity to single muscles, volumes of interest (VOI) were positioned double obliquely and chosen as large as possible, while fitting entirely within the respective muscle. This was done individually for each subject, using 25 transversal gradient echo MRI slices for voxel planning. The resulting average volumes were $\text{VOI}_{\text{SOL}} = 45 \pm 9 \text{ cm}^3$ ($66 \times 44 \times 16 \text{ mm}^3$) and $\text{VOI}_{\text{GM}} = 40 \pm 5 \text{ cm}^3$ ($63 \times 41 \times 16 \text{ mm}^3$). Typical voxel positions can be seen in Fig. 1a. Acquired spectra were processed with the jMRUI software package [25], using the AMARES time domain fit algorithm [26]. PCr and Pi signal intensities, representing the area under

the peak in the frequency domain, were normalized to baseline PCr concentrations. pH values were calculated from the chemical shift between Pi and PCr [6], and PCr recovery times τ_{PCr} were fitted mono-exponentially to the PCr recovery time course. Maximum oxidative capacity (Q_{max}) was calculated from τ_{PCr} and the end-exercise values PCr and pH, using the ADP driven model [27, 28], errors of Q_{max} were calculated by error propagation. SNR was quantified as the ratio of the PCr peak amplitude to the standard deviation (SD) of noise at around 10 ppm up-field from the PCr frequency (width of noise region: 1/8 of total bandwidth).

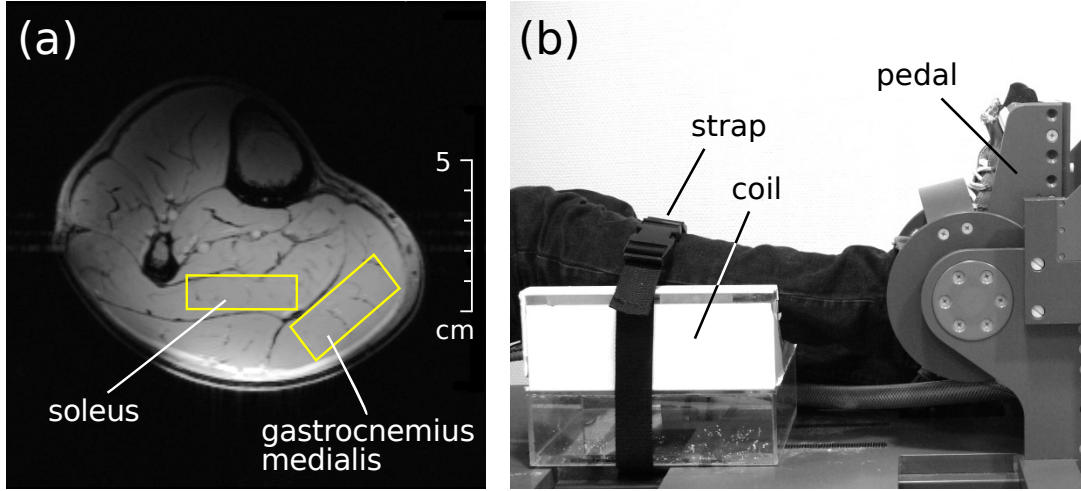


Fig. 1: (a) Typical position of the voxels in soleus and gastrocnemius medialis muscle, respectively, for localized ^{31}P MRS performed during two consecutive plantar flexion exercise bouts. (b) Coil position and shape, together with a fixation strap, helped to keep the calf in shape even during exercise with the ergometer.

The measurement protocol comprised 2 minutes at rest, during which time baseline data were acquired, 5 minutes of submaximal plantar flexion, and 7 minutes of recovery time. The isotonic exercise on a custom built MR compatible ergometer consisted of two consecutive pedal pushes between each period of MR data acquisition, which was every $T_R = 6$ seconds, i.e., the effective frequency of the exercise was 0.3 Hz. Maximum voluntary contraction force (MVC) of each subject was measured in the ergometer on the scanner bed, prior to the MRS measurements. The force of the exercises was set to 40 % of MVC, via the pressure in the air piston of the ergometer, and controlled throughout the experiment. The knee was straight and the calf was placed on the form-fitted array coil and fixed in position using a strap across the tibia (see Fig. 1b). Two equivalent exercise bouts were carried out, the first for measuring the time course of localized ^{31}P MR spectra in GM, and the second for SOL. They were separated by 28 minutes of inactivity (on average, minimum was 20 minutes), ensuring that PCr, Pi and pH values had fully recovered to basal levels at the beginning of the second bout.

Control experiments were performed in four subjects (two from the group performing the full protocol, and two additional subjects) by repeatedly measuring in SOL. The purpose of these measurements, was to assess the reproducibility of metabolite

quantification and fitting of τ_{PCr} at low PCr depletion in this muscle between subsequent exercise bouts, with a resting phase of 25 min. Day-to-day reproducibility was tested after one week in one subject.

Results

PCr and Pi were quantified from ^{31}P spectra acquired in time series with a temporal resolution of 6 s. The average SNR of PCr at rest was 64 ± 15 in SOL, and 83 ± 12 in GM. The mean force applied by the volunteers during exercise, as measured with the sensor on the ergometer pedal, was $40 \pm 10\%$ of MVC in the SOL bout, and $40 \pm 8\%$ of MVC in the GM bout. The mismatch between each individual's forces in the two exercise bouts was $1.8 \pm 1.3\%$ of MVC. All values relate to individual MVC.

Stack plots of ^{31}P -spectra from a single subject are shown in Fig. 2. Data are plotted without temporal averaging, representing the acquisition's full time resolution of 6 s. Time courses of PCr and Pi signal averaged over all 9 subjects are shown in Fig. 3. PCr depletion was detected in the soleus muscle of all subjects, and ranged from 6 % to 38 % at end of exercise. GM showed far stronger depletion in all subjects, ranging between 49 % and 94 %, which is consistent with [28]. Average end-exercise PCr depletions of SOL and GM can be read from Fig. 3 and are summarized in

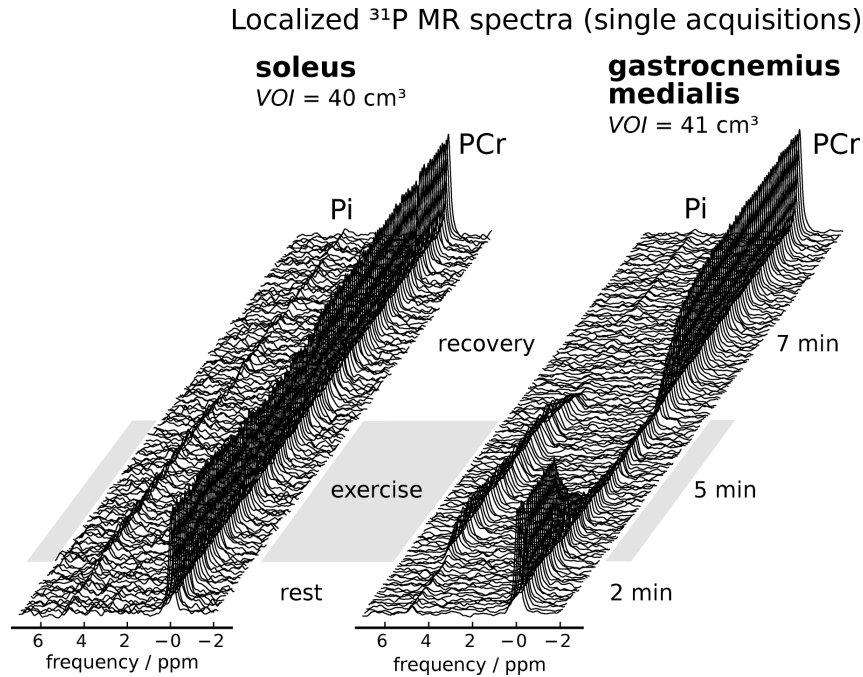


Fig. 2: Stack plots of spectra acquired in SOL (left) and GM (right) during rest, plantar flexion exercise (gray area) and recovery of one subject. Single-shot spectra ($T_R = 6$ s) are shown without averaging. Exponential line broadening of 25 Hz and zero filling ($8\times$) were applied for better visualization.

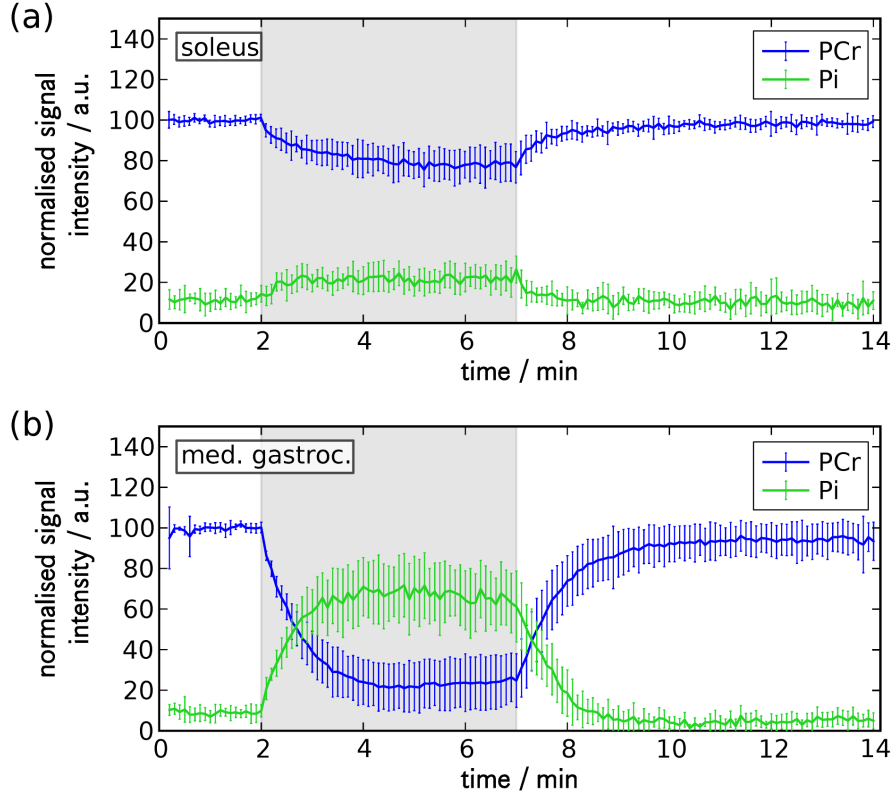


Fig. 3: PCr and Pi signal in (a) SOL and, for comparison, (b) GM at rest, during exercise (marked Gray) and during recovery, from two equivalent exercise bouts. Mean \pm SD of $n = 9$ subjects.

Table 1. The table also shows the average PCr recovery times τ_{PCr} , excluding the one subject with only 6 % depletion in SOL, due to insufficient dynamic range for the PCr recovery fit.

Intracellular pH was also quantified at a temporal resolution of 6 s. The time courses of pH in SOL (Fig. 4a) and GM (Fig. 4b), respectively, are shown as the average over all 9 subjects. Data points where the SNR of Pi was below 1.3 for individual subjects were not included. Average pH values at rest, end of exercise and the post-exercise minimum in SOL and GM are given in Table 1.

In SOL, pH increased immediately at the onset of exercise, rising by 0.03 ± 0.01 within 12 s, see Fig. 4a. The pH remained elevated throughout the exercise, with a maximum of 7.09 ± 0.02 . During recovery, pH returned to resting values within 23 ± 8 s and continued to decrease slightly below resting values by -0.016 ± 0.012 ($p < 0.005$ pre vs. post exercise pH), as quantified from 4 blocks of 5 averaged spectra at rest and during the last 2 minutes of the measurement. The pH evolution in SOL was in stark contrast to GM: the initial pH rise in the first 12 s was 0.07 ± 0.02 (see

Table 1: PCr depletion (relative to resting PCr signal), PCr recovery time constant τ_{PCr} , pH values at rest, at end of exercise and at the post exercise minimum and maximum oxidative capacity Q_{max} of $n = 9$ subjects. Data were quantified from unaveraged spectra, errors for PCr depletion and τ_{PCr} of individuals are SDs resulting from the fitting algorithm, the uncertainty of Q_{max} was derived via error propagation. The pH at the end of exercise and the post exercise minimum in GM were quantified from four unaveraged spectra, (SDs over five data points). The resting pH in SOL and GM and the pH during the last 2 min measured in SOL was derived from blocks of five accumulated spectra (SDs over four data points). Group averages represent the mean \pm SD of individuals' data.

	Subj.	PCr depletion	τ_{PCr}	pH _{rest}	pH _{end ex}	pH _{end rcv} (SOL) pH _{min} (GM)	Q_{max} [mM/min]
SOL	1	$6 \pm 1\%$	-	7.04 ± 0.004	7.05 ± 0.01	7.03 ± 0.006	-
	2	$38 \pm 2\%$	$54 \pm 5\text{ s}$	6.99 ± 0.014	7.03 ± 0.01	7.00 ± 0.010	23 ± 2
	3	$23 \pm 2\%$	$23 \pm 4\text{ s}$	7.03 ± 0.006	7.02 ± 0.02	6.99 ± 0.005	40 ± 7
	4	$17 \pm 1\%$	$20 \pm 3\text{ s}$	7.00 ± 0.002	7.02 ± 0.01	6.97 ± 0.014	39 ± 7
	5	$14 \pm 1\%$	$63 \pm 12\text{ s}$	7.02 ± 0.001	7.05 ± 0.01	7.00 ± 0.002	10 ± 2
	6	$20 \pm 3\%$	$24 \pm 7\text{ s}$	7.02 ± 0.003	7.08 ± 0.01	7.01 ± 0.002	33 ± 10
	7	$15 \pm 2\%$	$30 \pm 9\text{ s}$	7.02 ± 0.010	7.07 ± 0.01	7.00 ± 0.018	23 ± 7
	8	$11 \pm 1\%$	$77 \pm 15\text{ s}$	7.02 ± 0.006	7.06 ± 0.02	7.00 ± 0.012	8 ± 2
	9	$26 \pm 1\%$	$42 \pm 5\text{ s}$	7.02 ± 0.004	7.06 ± 0.01	7.01 ± 0.006	23 ± 2
GM	1	$65 \pm 1\%$	$32 \pm 1\text{ s}$	7.03 ± 0.003	7.03 ± 0.01	6.90 ± 0.05	51 ± 1
	2	$90 \pm 2\%$	$71 \pm 3\text{ s}$	6.98 ± 0.019	6.47 ± 0.03	6.38 ± 0.06	30 ± 1
	3	$94 \pm 1\%$	$68 \pm 1\text{ s}$	7.08 ± 0.003	6.58 ± 0.02	6.46 ± 0.03	30 ± 1
	4	$69 \pm 1\%$	$34 \pm 1\text{ s}$	7.01 ± 0.002	6.97 ± 0.02	6.80 ± 0.01	49 ± 1
	5	$69 \pm 1\%$	$62 \pm 2\text{ s}$	7.05 ± 0.010	6.78 ± 0.01	6.65 ± 0.10	29 ± 1
	6	$76 \pm 2\%$	$44 \pm 2\text{ s}$	7.04 ± 0.005	6.95 ± 0.03	6.83 ± 0.12	41 ± 2
	7	$49 \pm 1\%$	$45 \pm 1\text{ s}$	7.04 ± 0.004	7.01 ± 0.01	6.87 ± 0.02	31 ± 1
	8	$83 \pm 1\%$	$45 \pm 1\text{ s}$	7.05 ± 0.008	6.87 ± 0.01	6.68 ± 0.01	42 ± 1
	9	$73 \pm 2\%$	$37 \pm 2\text{ s}$	7.06 ± 0.007	6.93 ± 0.02	6.75 ± 0.03	48 ± 1
SOL		$19 \pm 9\%$	$37 \pm 17\text{ s}$	7.02 ± 0.02	7.06 ± 0.02	7.00 ± 0.01	25 ± 12
GM		$74 \pm 14\%$	$49 \pm 15\text{ s}$	7.04 ± 0.03	6.85 ± 0.19	6.70 ± 0.19	39 ± 9

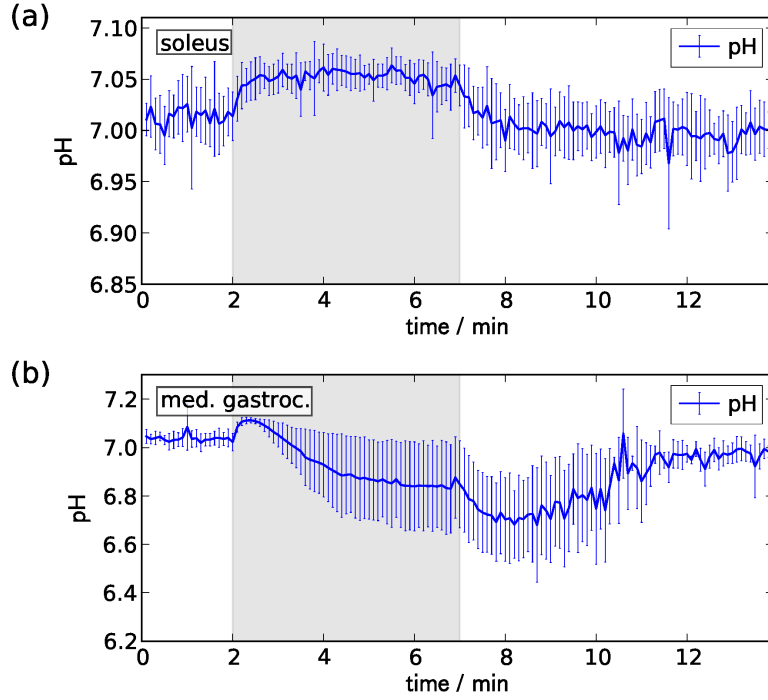


Fig. 4: Intracellular pH in (a) SOL and (b) GM with a time resolution of 6 s, mean \pm SD of all $n = 9$ subjects. Note the different scale of the two plots.

Fig. 4b), and the maximum of 7.12 ± 0.01 was reached after 23 ± 8 s. End-exercise pH in GM varied widely between subjects, ranging from 6.47 to 7.02 and was followed by a post-exercise drop of 0.15 ± 0.03 , before returning towards its resting value.

Two representative individual subjects' datasets are presented in Fig. 5, showing PCr time courses (Fig. 5a and b) with a temporal resolution of 6 s. For better visualization only, the pH is shown in Fig. 5c and d with 12 s time resolution, obtained by averaging two successive spectra at each data point. As for averaged data, points with $\text{SNR}(\text{Pi}) < 1.3$ were omitted in the individual pH graph.

To investigate possible effects on the measured Pi peak by low spatial resolution or a partial volume effect, retrospective spatial averages of spectra are compared to the original data. Fig. 6 (a) and (b) show spectra localized in SOL and GM, respectively, from unaveraged single-shot acquisitions, after 1 minute of exercise. To simulate partial volume effects, Fig. 6 (c) shows the average of the spectra from the two muscles, while Fig. 6 (d) shows a combined spectrum obtained by weighting SOL and GM data by 70:30. All data in Fig. 6 are from the same subject. Depending on the effective time interval of temporal averaging, the width and shape of the Pi peak also varies, corresponding to different derived pH (data not shown).

Results of the measurements repeated in the same subjects show good reproducibility of the applied force, which was adjusted to yield relatively low PCr depletion in

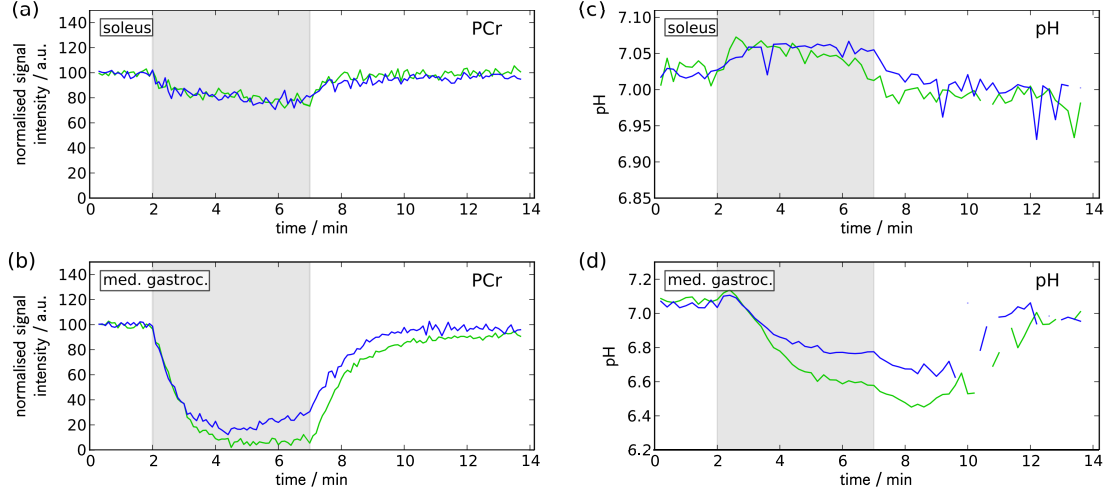


Fig. 5: Time courses of PCr signal and pH evolution of the same two representative subjects. The PCr signal in (a) SOL and (b) GM is shown with 6 s time resolution. The pH evolution shown in (c) for SOL and (d) for GM was derived from spectra after averaging two time points each (i.e., 12 s time resolution), datapoints with an SNR of the Pi peak below 1.3 are omitted. Note that the plots showing pH (c, d) are scaled differently.

SOL of 22 % and 26 % (group averages). Also the end-exercise pH in the neutral to slightly alkaline regime and PCr recovery time of 20 s vs. 27 s were reproducible (see Table 2) and not significantly different between bouts. PCr depletion and pH changes were also found to be reproducible in measurements repeated after one week.

These measurements also showed a small, significant pH decrease by -0.03 ± 0.02 , post vs. pre exercise, in all bouts. The pH measured during the 2 minutes before exercise was not significantly different between bout 1 and 2.

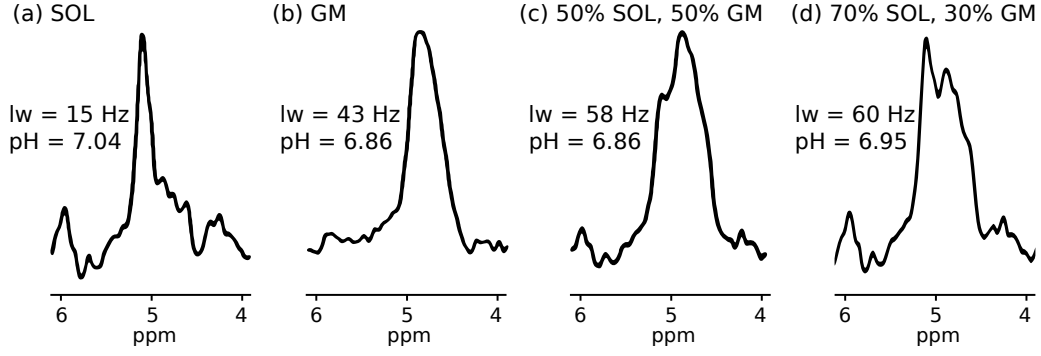


Fig. 6: Pi peaks in spectra from (a) SOL, (b) GM, and averages of the two datasets, (c) 50 % SOL and 50 % GM, (d) 70 % SOL and 30 % GM. All spectra were measured in the same subject, represent the same point in time (after 1 minute of exercise), and are scaled to the same amplitude. Linewidth (lw) and the calculated pH are given.

Table 2: Repeated measurements in SOL, for each subject with the same exercise intensity, respectively. Bouts one and two were spaced by 25 min of inactivity. The measurements on subject #10 were repeated after one week.

Subject	Bout	PCr depl.	τ_{PCr}	pH _{end}	Force / N
#6	1	48 ± 2 %	27 ± 2 s	6.92 ± 0.03	243 ± 14
	2	34 ± 2 %	34 ± 3 s	6.98 ± 0.02	234 ± 15
#9	1	18 ± 2 %	17 ± 4 s	7.04 ± 0.01	255 ± 22
	2	12 ± 2 %	19 ± 7 s	7.04 ± 0.01	222 ± 16
#10	1	3 ± 2 %	-	7.07 ± 0.01	291 ± 11
	2	4 ± 2 %	-	7.07 ± 0.02	292 ± 10
#11	1	36 ± 1 %	15 ± 2 s	7.06 ± 0.01	285 ± 24
	2	39 ± 2 %	28 ± 3 s	7.06 ± 0.01	283 ± 29
Mean	1	26 ± 20 %	20 ± 6 s	7.02 ± 0.07	267 ± 21
	2	22 ± 17 %	27 ± 7 s	7.04 ± 0.04	256 ± 32

Measurement repeated after 1 week

Subject	Bout	PCr depl.	τ_{PCr}	pH _{end}	Force / N
#10	1	6 ± 2 %	-	7.10 ± 0.02	284 ± 9
	2	4 ± 4 %	-	7.11 ± 0.03	283 ± 11

Discussion

This study successfully shows that quantification of PCr, Pi and pH is feasible with high specificity, even in the deeper lying human soleus muscle, by combining high temporal resolution of 6s with spatial selectivity. This was achieved by exploiting the high SNR of ^{31}P spectra acquired with a semi-LASER sequence, using a custom-built form-fitted array coil [23] on a 7T MR scanner, in combination with a plantar flexion paradigm.

SOL consistently showed PCr depletion, although at far lower levels than GM. The time courses of pH differed even qualitatively: sharing a similar rise at the beginning of exercise, pH in SOL remained alkaline during the exercise and dropped towards basal levels shortly after the end of exercise. In GM however, pH was declining throughout the exercise, with a further drop post-exercise. This is consistent with ASL data from Schewzow et al. [29], where perfusion in GM increased much more than in SOL in a comparable exercise paradigm. In a previous study [15], simple acquisition of FID vs. a localization scheme was compared, using the same standard single loop coil in both measurements, demonstrating significantly different results from the two methods. The results from the present study indicate that contamination from the lesser activated SOL is a possible source of bias for quantification of PCr, Pi and consequently pH in unlocalized experiments. This emphasizes the importance of spatial localization in order to provide a more specific interpretation of the muscle under investigation.

Average PCr recovery times τ_{PCr} in SOL were shorter than in GM. Acidification slows down PCr recovery in muscle tissue [30, 31], therefore the maximum oxidative capacity Q_{max} is a more suitable measure to compare recovery from exercise in muscles with different pH. This parameter was also comparable between SOL and GM, but slightly lower in SOL. Nevertheless, it has to be taken into account that the two muscles were working in a different metabolic regime, SOL at low activation and alkaline pH working mainly aerobic, and GM at much higher activation and acidification with a high glycolytic contribution. A sound comparison of these muscles would require similar PCr depletion and end-exercise pH values, e.g., via multiple measurements at different exercise intensities, which is beyond the scope of this study.

The reproducibility measurements show good agreement of data acquired from SOL in two bouts on the same day (see Table 2). The stability of mean forces indicates that the subjects were exercising at a comparable level in both bouts, and similar end-exercise values of PCr depletion and pH show that SOL was also activated to nearly the same extent. τ_{PCr} showed small variation from bout to bout in subjects #6 and #9, with larger variability in subject #11, the differences from bout to bout were not statistically significant. All recovery times in SOL were in the lower range of all measurements in this study and hence distinct from values typically measured in GM. When testing day-to-day reproducibility over the course of one week, PCr depletion was consistently very low and pH was elevated throughout the exercise in SOL on both days and in all exercise bouts, which were performed with the same force (see Table 2, subject #10). Reproducing the same effect of exercise (i.e., equal activation of SOL and hence PCr depletion) by repeating the measurements after

a longer period of several months was attempted in three subjects and found to be challenging. Possible reasons for larger variability (data not shown) are that the subjects may have distributed the exercise load to individual calf muscles differently, when asked to perform the same exercise after a long time, and that training state and living circumstances can change over longer periods [32], which could influence the measured parameters. Yet, all measurements performed to test reproducibility in SOL resulted in values that corresponded to low metabolic activation, which confirms that the striking differences observed in data from SOL and GM were not caused by repeating the exercise within 25 min, but represent intrinsic differences in the metabolic response of these muscles to the same exercise. This was also consistent with previous studies [15,33], which indicate that repeating exercise has no severe (if any) influence on PCr recovery kinetics, after a sufficiently long phase of inactivity. This applies in particular to SOL which was activated only modestly.

The main advantage of the semi-LASER sequence is that the size and orientation of the single voxel can be explicitly defined in all three dimensions. Consequently, a large voxel can be selected, anatomically matched to the muscle, which minimizes partial volume effects. Therefore, the method has high specificity [20], yields good SNR and, as a single-shot sequence, allows high temporal resolution. Together, this is greatly beneficial for measurements in a superficial muscle like GM. Furthermore it forms the basis of an inherent virtue of the semi-LASER sequence: the ability to penetrate into deeper lying tissues and afford accurate, localized data. Obviously, in deeper areas localization via a small coil is not applicable, and the location and non-trivial geometry of a muscle like SOL make it particularly inaccessible, even to other localization methods. With a 2D ISIS-like sequence for instance, as used in [9], placing voxels in SOL without overlap to GM or GL is nearly impossible.

Quantification of fast pH changes requires high temporal resolution, e.g., to follow the immediate pH increase at the onset of exercise. In GM, the average time to maximum pH was 23 s, and some subjects showed a similarly fast increase of pH in SOL. Such dynamics can only be resolved with a temporal resolution of 11 s or better, to avoid undersampling. Also the quantification of the PCr recovery time constant τ_{PCr} greatly benefits from higher temporal resolution. Particularly at low depletions, a sufficient number of data points needs to be acquired while PCr concentration is still significantly below resting values, i.e., the low dynamic range necessitates high time resolution. Aided by the temporal resolution of 6 s, the feasibility of τ_{PCr} quantification at PCr depletions as low as 15 % was demonstrated in this study.

The initial pH rise supports the notion that in the first seconds of exercise PCr breakdown is the dominant mechanism to ATP production, with mitochondrial activity not being elevated beyond resting activity, and minimal glycolytic contribution. The alkaline pH throughout the exercise in SOL suggests that the ATP need can be met by PCr breakdown and oxidative phosphorylation [27], which is in agreement with the modest PCr depletion rates. A small decrease of post exercise pH below pre exercise levels in SOL was found within all groups (i.e., with the full exercise protocol and in reproducibility measurements), which can be explained by the proton production associated with oxidative ATP synthesis after aerobic exercise.

The elevated pH in SOL also affirms that the PCr decrease (and Pi increase) is a physiologic effect and not due to a motion artifact or contamination from strongly

depleted adjacent muscles, since this would be accompanied by a pH drop or a split Pi peak. Contamination is a form of spatial averaging across two muscles, which can result in artifacts of the apparent Pi peak, regarding position, width and shape, when the muscles are in different metabolic states. Consequently the resulting value of pH can lie anywhere between the actual pH values of the respective muscles, depending on the volume fraction of the muscles in the averaged volume (see Fig. 6c and d). This bias of pH can also vary with time, due to the different metabolic evolution of the muscles during exercise. Also temporal averaging can be a source of artifacts, as the Pi peak moves in frequency, when pH changes over time. With low temporal resolution this is perceived as an increased Pi linewidth, or when the (averaged) acquisition is sufficiently long compared to the pH shift, even might appear as two components in the broad peak.

To summarize, accurate spatial localization and sufficiently high temporal resolution help to establish a more reliable, precise and accurate quantification of Pi and hence pH, specific to a particular muscle.

Conclusion

Localized ^{31}P MR spectra were acquired from the deeper lying soleus muscle at high temporal resolution during and after exercise. The time courses of PCr and pH indicate lower activation of SOL than the neighboring GM in this form of exercise. The high temporal resolution is the basis for quantification of fast pH changes, e.g., the initial rise of pH which can be on the order of 10 s. Furthermore, high temporal resolution is desirable to improve quantification of PCr recovery, and to avoid erroneous Pi peak broadening, by minimizing temporal averaging over shifting metabolite peaks. All together, this work illustrates the relevance and effect of high temporal resolution and accurate spatial localization, enabling quantification of fast or subtle metabolic processes, as well as improving specificity in many regards.

Acknowledgments:

This work has been supported by the Austrian BMWFJ, FFG Project #832107, “Vienna Research Studio for Ultra-High Field Magnetic Resonance Applications”, Austrian Science Fund (FWF): J 3031-N20, I1743-B13 and an unrestricted grant to Ewald Moser funded by Siemens Medical.

Conflict of interest:

The authors declare that they have no conflict of interest.

Ethical standards:

The study has been approved by the local ethics committee and has therefore been performed in accordance with the ethical standards of the 1964 Declaration of Helsinki and

its later amendments. All subjects gave informed consent in writing before being included in the study.

References

- [1] Hoult DI, Busby SJ, Gadian DG, Radda GK, Richards RE, Seeley PJ (1974) Observation of tissue metabolites using ^{31}P nuclear magnetic resonance. *Nature* 252:285–287
- [2] Chance B, Im J, Nioka S, Kushmerick M (2006) Skeletal muscle energetics with PNMRS: personal views and historic perspectives. *NMR Biomed* 19:904–926
- [3] Bendahan D, Giannesini B, Cozzzone PJ (2004) Functional investigations of exercising muscle: a noninvasive magnetic resonance spectroscopy-magnetic resonance imaging approach. *Cell Mol Life Sci* 61:1001–1015
- [4] Prompers JJ, Jeneson JA, Drost MR, Oomens CC, Strijkers GJ, Nicolay K (2006) Dynamic MRS and MRI of skeletal muscle function and biomechanics. *NMR Biomed* 19:927–953
- [5] Kemp GJ, Meyerspeer M, Moser E (2007) Absolute quantitation of phosphorus metabolite concentrations in human muscle in vivo by ^{31}P MRS: a quantitative review. *NMR Biomed* 20:555–565
- [6] Moon RB, Richards JH (1973) Determination of intracellular pH by ^{31}P MR. *J Biol Chem* 248:7276–7278
- [7] Gray H, Pick TP, Howden R (eds.) (1995) *Gray’s Anatomy*. 15th edition, Barnes & Noble Books, New York
- [8] Price TB, Kamen G, Damon BM, Knight CA, Applegate B, Gore JC, Eward K, Signorile JF (2003) Comparison of MRI with EMG to study muscle activity associated with dynamic plantar flexion. *Magn Reson Imaging* 21:853–861
- [9] Vandenborne K, Walter G, Leigh JS, Goelman G (1993) pH heterogeneity during exercise in localized spectra from single human muscles. *Am J Physiol* 265:C1332–1339
- [10] Noseworthy MD, Bulte DP, Alfonsi J (2003) BOLD magnetic resonance imaging of skeletal muscle. *Semin Musculoskelet Radiol* 7:307–315
- [11] Vandenborne K, Walter G, Ploutz-Snyder L, Dudley G, Elliott MA, Meirleir KD (2000) Relationship between muscle T2* relaxation properties and metabolic state: a combined localized ^{31}P -spectroscopy and ^1H -imaging study. *Eur J Appl Physiol* 82:76–82
- [12] Jacobi B, Bongartz G, Partovi S, Schulte AC, Aschwanden M, Lumsden AB, Davies MG, Loebe M, Noon GP, Karimi S, Lyo JK, Staub D, Huegli RW, Bilecen D (2012) Skeletal muscle BOLD MRI: from underlying physiological concepts to its usefulness in clinical conditions. *J Magn Reson Imaging* 35:1253–1265

- [13] Layec G, Malucelli E, Fur YL, Manners D, Yashiro K, Testa C, Cozzzone PJ, Iotti S, Bendahan D (2013) Effects of exercise-induced intracellular acidosis on the phosphocreatine recovery kinetics: a ^{31}P MRS study in three muscle groups in humans. *NMR Biomed* 26:1403–1411
- [14] Forbes SC, Slade JM, Francis RM, Meyer RA (2009) Comparison of oxidative capacity among leg muscles in humans using gated ^{31}P 2-D chemical shift imaging. *NMR Biomed* 22:1063–1071
- [15] Meyerspeer M, Robinson S, Nabuurs CI, Scheenen T, Schoisengeier A, Unger E, Kemp G, Moser E (2012) Comparing localized and nonlocalized dynamic ^{31}P magnetic resonance spectroscopy in exercising muscle at 7T. *Magn Reson Med* 68:1713–1723
- [16] Davis AD, Noseworthy MD (2013) Consistency of Post-Exercise Skeletal Muscle BOLD Response. In: *Proceedings of the 21st scientific meeting, International Society for Magnetic Resonance in Medicine, Salt Lake City*, p 1640
- [17] Allen PS, Matheson GO, Zhu G, Gheorgiu D, Dunlop RS, Falconer T, Stanley C, Hochachka PW (1997) Simultaneous ^{31}P MRS of the soleus and gastrocnemius in Sherpas during graded calf muscle exercise. *Am J Physiol* 273:R999–1007
- [18] Valkovič L, Chmelík M, Kukurová IJ, Jakubová M, Kipfelsberger MC, Krumpolec P, Jelenc MT, Bogner W, Meyerspeer M, Ukropec J, Frollo I, Ukropcová B, Trattnig S, Krššák M (2014) Depth-resolved surface coil MRS (DRESS)-localized dynamic ^{31}P -MRS of the exercising human gastrocnemius muscle at 7T. *NMR Biomed* 27:1346–1352
- [19] Meyerspeer M, Krššák M, Kemp GJ, Roden M, Moser E (2005) Dynamic interleaved $^1\text{H}/^{31}\text{P}$ STEAM MRS at 3 Tesla using a pneumatic force-controlled plantar flexion exercise rig. *Magn Reson Mater Phy* 18:257–262
- [20] Meyerspeer M, Scheenen T, Schmid AI, Mandl T, Unger E, Moser E (2011) Semi-LASER-Localized Dynamic ^{31}P Magnetic Resonance Spectroscopy in Exercising Muscle at Ultrahigh Magnetic Field. *Magn Reson Med* 65:1207–1215
- [21] Bogner W, Chmelík M, Schmid AI, Moser E, Trattnig S, Gruber S (2009) Assessment of ^{31}P relaxation times in the human calf muscle: a comparison between 3 T and 7 T in vivo. *Magn Reson Med* 62:574–582
- [22] Parasoglou P, Xia D, Chang G, Regatte RR (2013) Dynamic three-dimensional imaging of phosphocreatine recovery kinetics in the human lower leg muscles at 3T and 7T: a preliminary study. *NMR Biomed* 26:348–356
- [23] Goluch S, Kuehne A, Meyerspeer M, Kriegl R, Schmid AI, Fiedler GB, Herrmann T, Mallow J, Hong SM, Cho ZH, Bernarding J, Moser E, Laistler E (2014) A form-fitted three channel ^{31}P , two channel ^1H transceiver coil array for calf muscle studies at 7T. *Magn Reson Med* doi: 10.1002/mrm.25339
- [24] Scheenen TW, Heerschap A, Klomp DW (2008) Towards ^1H -MRSI of the human brain at 7T with slice-selective adiabatic refocusing pulses. *Magn Reson Mater Phy* 21:95–101

- [25] Naressi A, Couturier C, Devos JM, Janssen M, Mangeat C, de Beer R, Graveron-Demilly D (2001) Java-based graphical user interface for the MRUI quantitation package. *Magn Reson Mater Phy* 12:141–152
- [26] Vanhamme L, van den Boogaart A, van Huffel S (1997) Improved method for accurate and efficient quantification of MRS data with use of prior knowledge. *J Magn Reson* 129:35–43
- [27] Kemp GJ, Radda GK (1994) Quantitative interpretation of bioenergetic data from ^{31}P and ^1H magnetic resonance spectroscopic studies of skeletal muscle: an analytical review. *Magn Reson Q* 10:43–63
- [28] Schmid AI, Schewzow K, Fiedler GB, Goluch S, Laistler E, Wolzt M, Moser E, Meyerspeer M (2014) Exercising calf muscle T_2^* changes correlate with pH, PCr recovery and maximum oxidative phosphorylation. *NMR Biomed* 27:553–560
- [29] Schewzow K, Fiedler GB, Meyerspeer M, Goluch S, Laistler E, Wolzt M, Moser E, Schmid AI (2015) Dynamic ASL and T_2^* -weighted MRI in exercising calf muscle at 7 T – a feasibility study. *Magn Reson Med* 73:1190–1195
- [30] Iotti S, Lodi R, Frassinetti C, Zaniol P, Barbiroli B (1993) In vivo assessment of mitochondrial functionality in human gastrocnemius muscle by ^{31}P MRS. The role of pH in the evaluation of phosphocreatine and inorganic phosphate recoveries from exercise. *NMR Biomed* 6:248–253
- [31] Kemp GJ, Taylor DJ, Radda GK (1993) Control of phosphocreatine resynthesis during recovery from exercise in human skeletal muscle. *NMR Biomed* 6:66–72
- [32] Hoff E, Brechtel L, Strube P, Konstanczak P, Stoltenburg-Didinger G, Perka C, Putzier M (2013) Noninvasive monitoring of training induced muscle adaptation with ^{31}P -MRS: fibre type shifts correlate with metabolic changes. *Biomed Res Int* doi:10.1155/2013/417901
- [33] Baligand C, Wary C, Ménard JC, Giacomini E, Hogrel JY, Carlier PG (2011) Measuring perfusion and bioenergetics simultaneously in mouse skeletal muscle: a multi-parametric functional-NMR approach. *NMR Biomed* 24:281–290